Slope stability analysis based on improved radial movement optimization considering seepage effect

Jin, L., Wei, J., Luo, C., & Qin, T. (2023). Slope stability analysis based on improved radial movement optimization considering seepage effect. Alexandria Engineering Journal, 79, 591-607.

Presenter: Jia-Yi Wu

Advisor: Prof. Jia-Jyun Dong

Date: 2023/12/01

Outlines

Introduction

- Slope stability analysis constitutes an important geotechnical problem.
- The limit equilibrium methods (LEMs) have been widely used and developed for estimate the minimum Factor of safety (Fs) associated with critical failure surface (CFS) in engineering practice.
- The traditional search optimization methods, like grid search method, variation method, simplex method, conjugate-gradient method, random search method and Monte Carlo method.
- Many optimization algorithms have been adopted and developed to solve this problem, but none of them can combine all the advantages of these algorithms.

Optimization method	Advantages	Disadvantages
Genetic Algorithm (GA)	Search flexibility, high applicability	Low efficiency, easy premature, difficulty to selectparameters
Simulated Annealing Algorithm (SA)	High precision, application simple	Low efficiency, sensitivity for initialization
Particle Swarm Optimization (PSO)	Application simple, high efficiency	Poor precision, poor stability
Ant Colony Optimization (ACO)	Application simple, high precision	Low efficiency
Artificial Fish Swarms Algorithm (AFS)	High efficiency	Poor precision
Gravitational Search Algorithm (GS)	Application simple	Unknown
Evolutional Programming (EP)	Application simple	Low efficiency, sensitivity for initialization
Black Hole Algorithm (BHA)	High efficiency, Application simple	Premature convergence
Harmony Search Algorithm (HM)	High efficiency for small-scale problem	low efficiency for complicated problem
Biogeography-based Optimization (BBO)	High precision, high stability	Unknown
Cuckoo search	High efficiency	Hard to convergence

- Radial Movement Optimization algorithm (RMO) is a newly proposed algorithm with the advantages in simple progress.
- Improved Radial Movement Optimization algorithm (IRMO) has showed great effectiveness and accuracy.
- The instability of most natural slopes is closely related to the influence of groundwater.
- The simplification or simulation of seepage field is generally the essential step before computation due to the complexity of seepage mechanism and difficult actual-seepage field drawing.

Slope stability analysis considering seepage

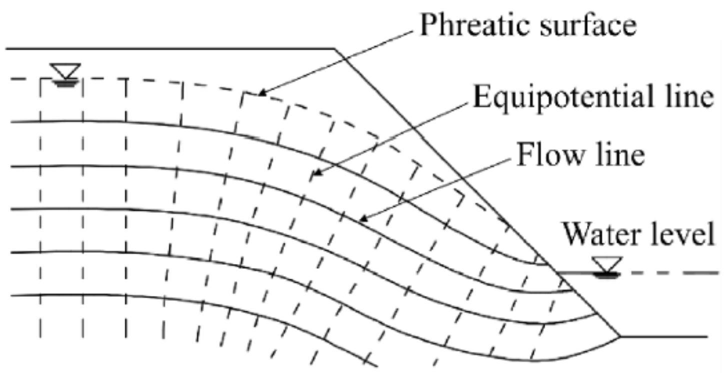

(a) Actual seepage field

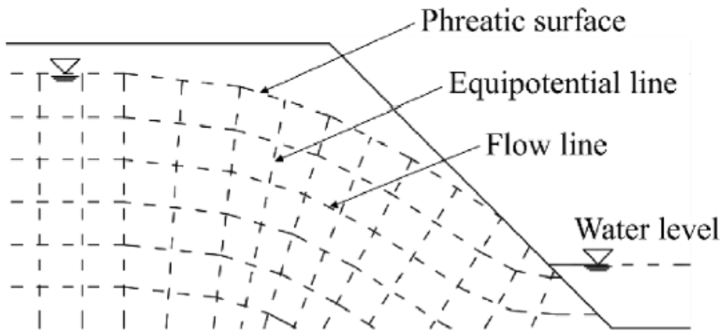

(b) Simplified seepage field

- Streamlines and equipotential lines intersect perpendicularly to each other to form a flow net in slope.
- The lines are commonly simplified in a reasonable form for infiltration force analysis.

- Simplied phreatic surfaces could be fitted by multi-segments associated with divided strips to simulate actual phreatic surfaces.

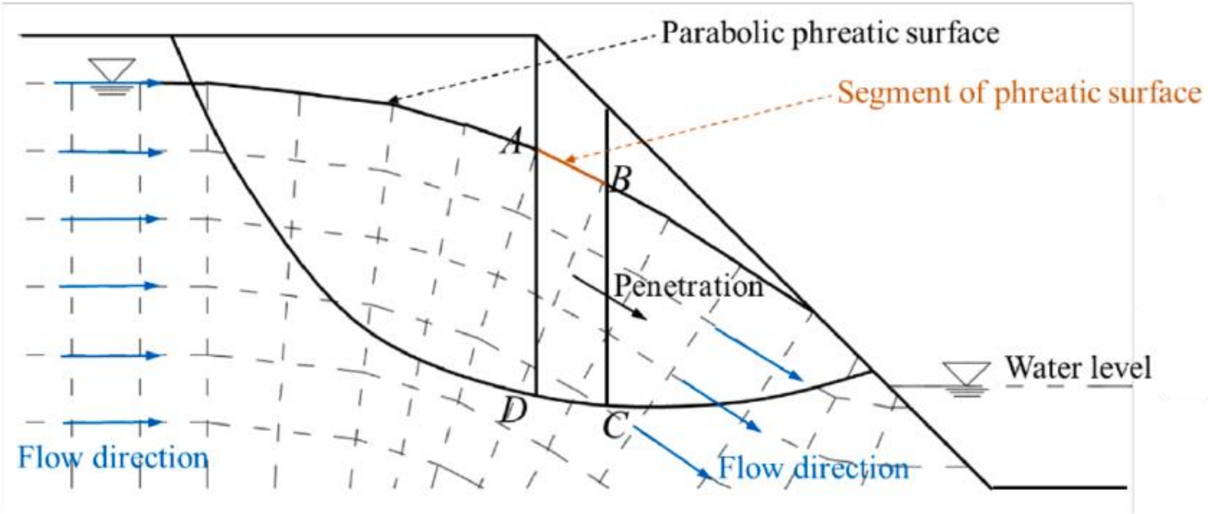

- First the slide body is divided into strips.
- Analyzing the reaction force of the infiltration force.

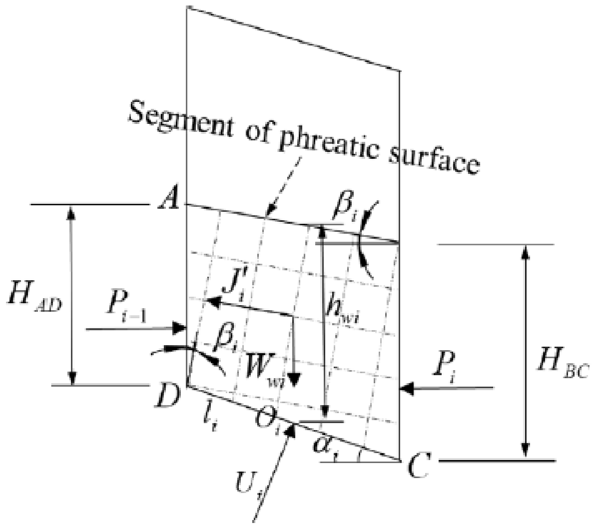

- Static equilibrium

In horizontal direction

$$U_i \sin\alpha_i - J'_{ix} + P_{i-1} - P_i = 0$$

In vertical direction

$$W_{wi} - U_i \cos\alpha_i - J_{iy} = 0$$

Coefficient calculation equation.

$$\begin{cases} U_i = \gamma_w l_i h_{wi} \cos^2\beta_i \\ P_i = \frac{1}{2}\gamma_w H_{BC}^2 \cos^2\beta_i \\ P_{i-1} = \frac{1}{2}\gamma_w H_{AD}^2 \cos^2\beta_i \end{cases}$$

P_i, P_{i-1} : the pore water pressure at the side of strip

H_{AD}, H_{BC} : the heights of the phreatic surface at the side of strip

U_i : the pore water pressure at strip base

h_{wi} : the average height of phreatic surface

β_i : the phreatic surface inclination

α_i : the base inclination

l_i : the base length of strip

J'_i : the reacting force of infiltration force

W_{wi}: the water weight

$$J'_{ix} = \gamma_w h_{wi} \cos^2\beta_i (H_{AD} - H_{BC} + l_i \sin\alpha_i)$$

$$J'_{iy} = \gamma_w h_{wi} \sin^2\beta_i l_i \cos\alpha_i$$

J'_{ix} : The J'$_i$ in x direction

J'_{iy} : The J'$_i$ in y direction

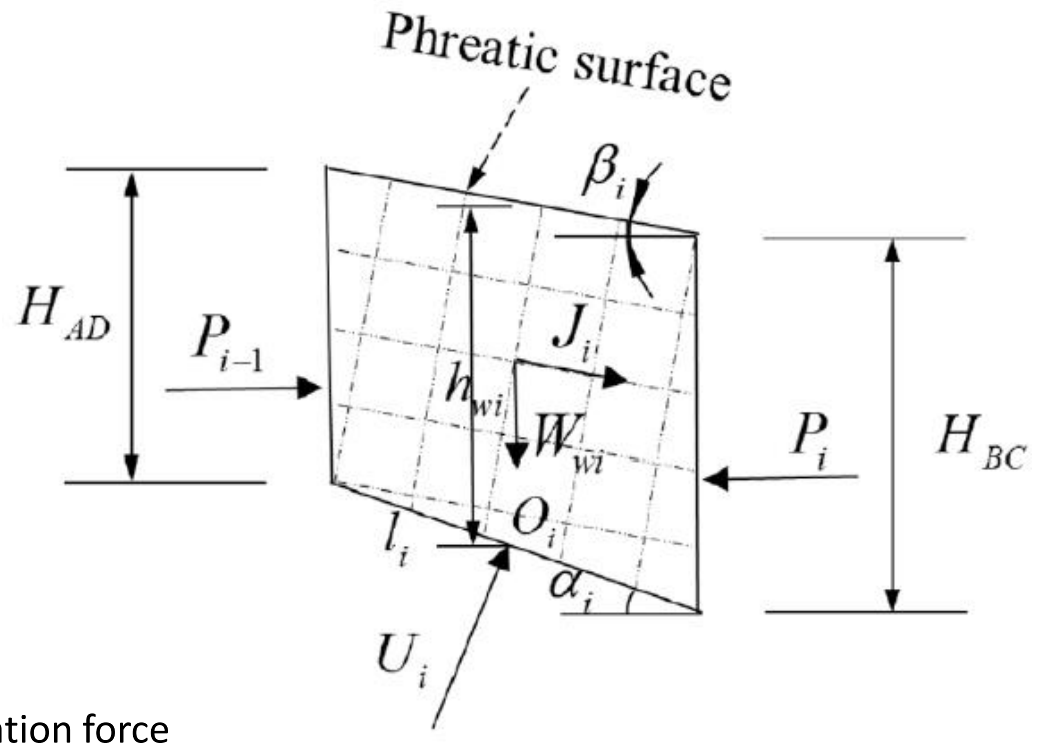

$$\frac{J'_{iy}}{J'_{ix}} = \tan\beta_i$$

$$J'_i = \frac{J'_{iy}}{\sin\beta_i} = \gamma_w h_{wi} l_i \sin\beta_i \cos\alpha_i$$

$$J_i = -J'_i = -\gamma_w h_{wi} l_i \sin\beta_i \cos\alpha_i$$

J'_i : the reacting force of infiltration force

β_i : the phreatic surface inclination

α_i : the base inclination

Calculate the moment at the bottom centre of strip O_i, and obtain the following from moment balance

$$P_{i-1}\left(\frac{1}{3}H_{i-1}+\frac{1}{2}l_i\sin\alpha_i\right)-P_i\left(\frac{1}{3}H_i-\frac{1}{2}l_i\sin\alpha_i\right)-J_i\cos\beta_i L_y=0$$

$$L_y=\frac{P_{i-1}\left(\frac{1}{3}H_{i-1}+\frac{1}{2}l_i\sin\alpha_i\right)-P_i\left(\frac{1}{3}H_i-\frac{1}{2}l_i\sin\alpha_i\right)}{J_i\cos\beta_i}$$

L_y : the location of infiltration force

As the width of strip is small enough, it could be considered that $H_i = H_{i-1} = h_{wi}$

$$L_y=\frac{1}{2}h_{wi}$$

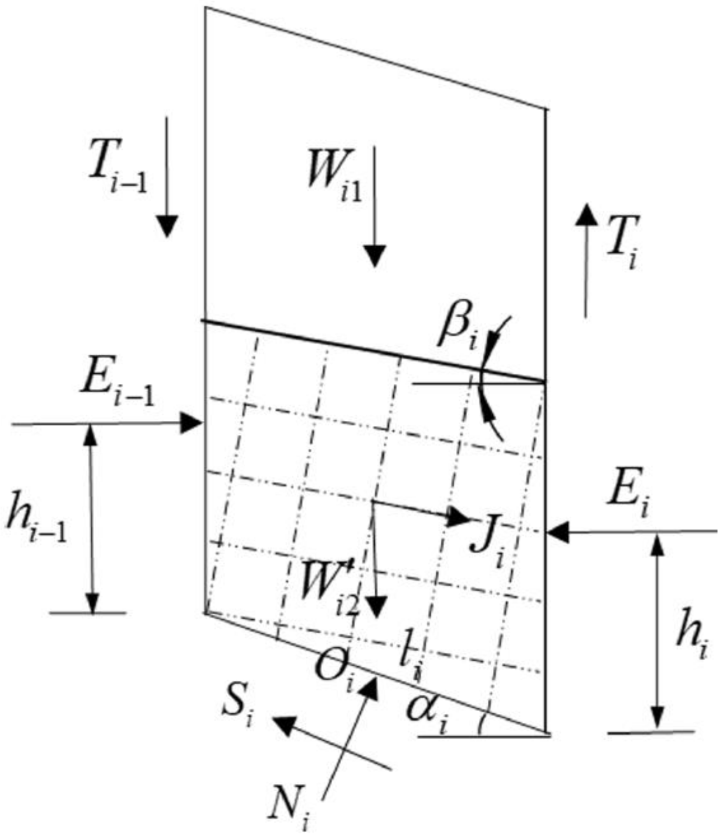

$$\Delta E_i = \left(W_{i1} + W_{i2}^{'} - \Delta T_i\right)\tan\alpha_i + J_i\sin\beta_i\tan\alpha_i + J_i\cos\beta_i$$

$$-\frac{\sec^2\alpha_i}{F_s + \tan\varphi_i\tan\alpha_i}\left[\left(W_{i1} + W_{i2}^{'} - \Delta T_i\right)\tan\varphi_i + J_i\sin\beta_i\tan\varphi_i + c_i l_i\cos\alpha_i\right]$$

$$T_i = \frac{J_i h_{wi}\cos\beta_i}{2l_i\cos\alpha_i} - \frac{\left[E_i(h_i - h_{i-1} - l_i\sin\alpha_i) + \Delta E_i\left(h_{i-1} + \frac{1}{2}l_i\cos\alpha_i\tan\alpha_i\right)\right]}{l_i\cos\alpha_i}$$

$$\Delta T_i = T_i - T_{i-1}$$

E_i, E_{i-1}: The normal forces at the side of strip

T_i, T_{i-1}: The shear forces at the side of strip

W_{i1}: The portion weight of strip above phreatic surface

W'_{i2}: The float weight of strip below phreatic surface

N_i: The contact pressure at strip base

S_i: The shear force at strip base

φ_i: The internal friction angle

c_i: The cohesion

β_i : the phreatic surface inclination

α_i : the base inclination

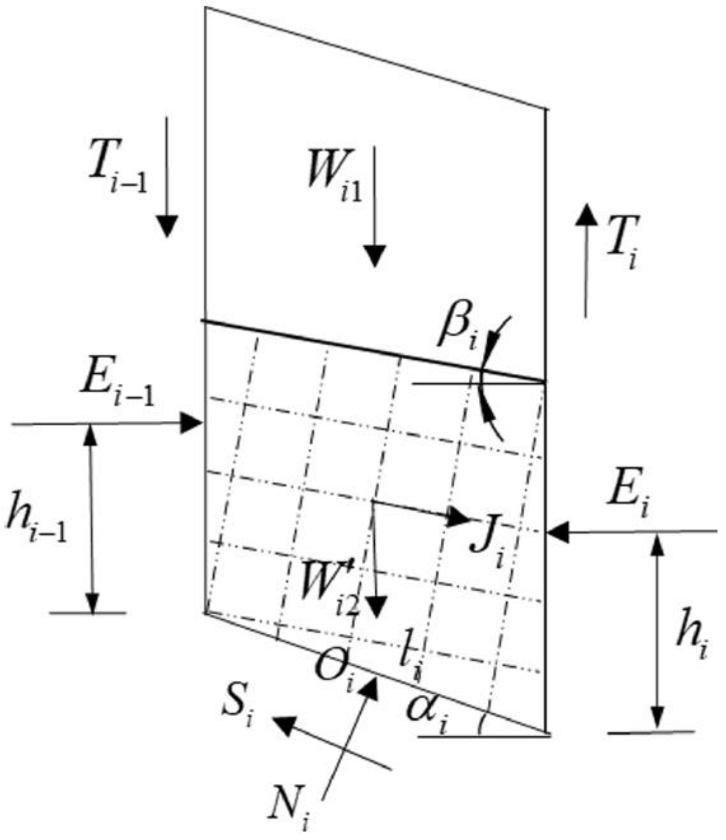

There is no external force acting on the assumed slide body, all of the increments of normal forces could be offset to zero.

$$\sum \Delta E_i = \sum \left(A_i - \frac{B_i}{F_s + \tan\varphi_i \tan\alpha_i} \right) = 0$$

$$A_i = \left(W_{i1} + W_{i2}^{'} - \Delta T_i\right)\tan\alpha_i + J_i \sin\beta_i \tan\alpha_i + J_i \cos\beta_i$$

$$B_i = \sec^2\alpha_i \cdot \left[c_i l_i \cos\alpha_i + \left(W_{i1} + W_{i2}^{'} - \Delta T_i\right)\tan\varphi_i + J_i \tan\varphi_i \sin\beta_i\right]$$

Fs = Factor of safety

W_{i1}: The portion weight of strip above phreatic surface

W'_{i2}: The float weight of strip below phreatic surface

N_i: The contact pressure at strip base

S_i: The shear force at strip base

φ_i: The internal friction angle

c_i: The cohesion

β_i : the phreatic surface inclination

α_i : the base inclination

Improved Radial Movement Optimization (IRMO)

$$X_{M,N} = \begin{bmatrix} x_{1,1} & x_{1,2} & \cdots & x_{1,N-1} & x_{1,N} \\ x_{2,1} & x_{2,2} & \cdots & x_{2,N-1} & x_{2,N} \\ \vdots & \vdots & \ddots & \vdots & \vdots \\ x_{M,1} & x_{M,2} & \cdots & x_{M,N-1} & x_{M,N} \end{bmatrix}$$

$$x_{i,j} = \min x_j + rand(0,1) \times (\max x_j - \min x_j)$$

In this study, C_1 and C_2 are set 0.4 and 0.5 respectively in advance.

$$Centre^k = Centre^{k-1} + C_1(Gbest - Centre^{k-1}) + C_2(Rbest^{k-1} - Centre^{k-1})$$

$Centre^k$: The central position

Gbest : Global optimal position

Non-circular critical failure surface in IRMO

$$[X_{M,N}] = \begin{bmatrix} d_1 & \alpha_{1,1} & \Delta\alpha_{1,2} & \cdots & \Delta\alpha_{1,N} \\ d_2 & \alpha_{2,1} & \Delta\alpha_{2,2} & \cdots & \Delta\alpha_{2,N} \\ \vdots & \vdots & \vdots & \ddots & \vdots \\ d_M & \alpha_{M,2} & \Delta\alpha_{M,2} & \cdots & \Delta\alpha_{M,N} \end{bmatrix}$$

d : The position of the upper entry point

α_1: The inclination angle between the first segment base and vertical direction,

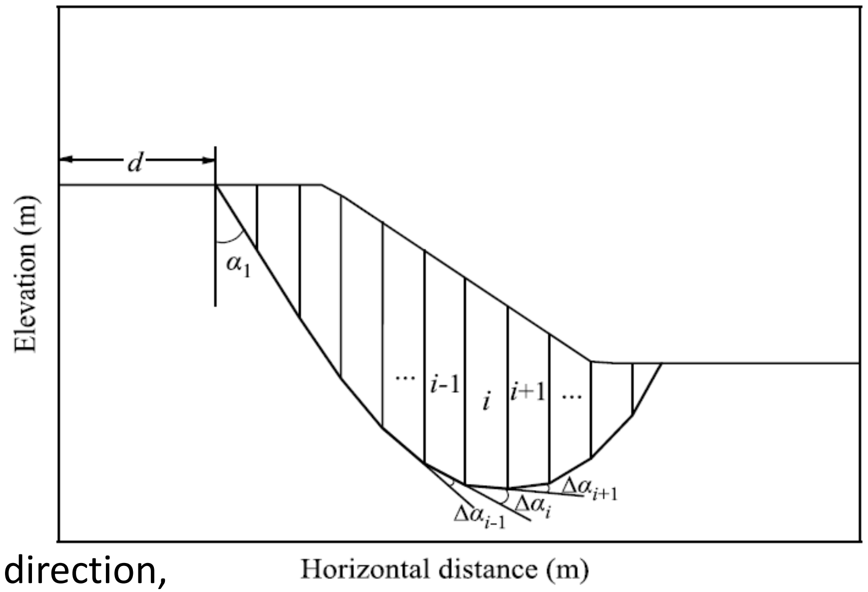

Results and Discussion

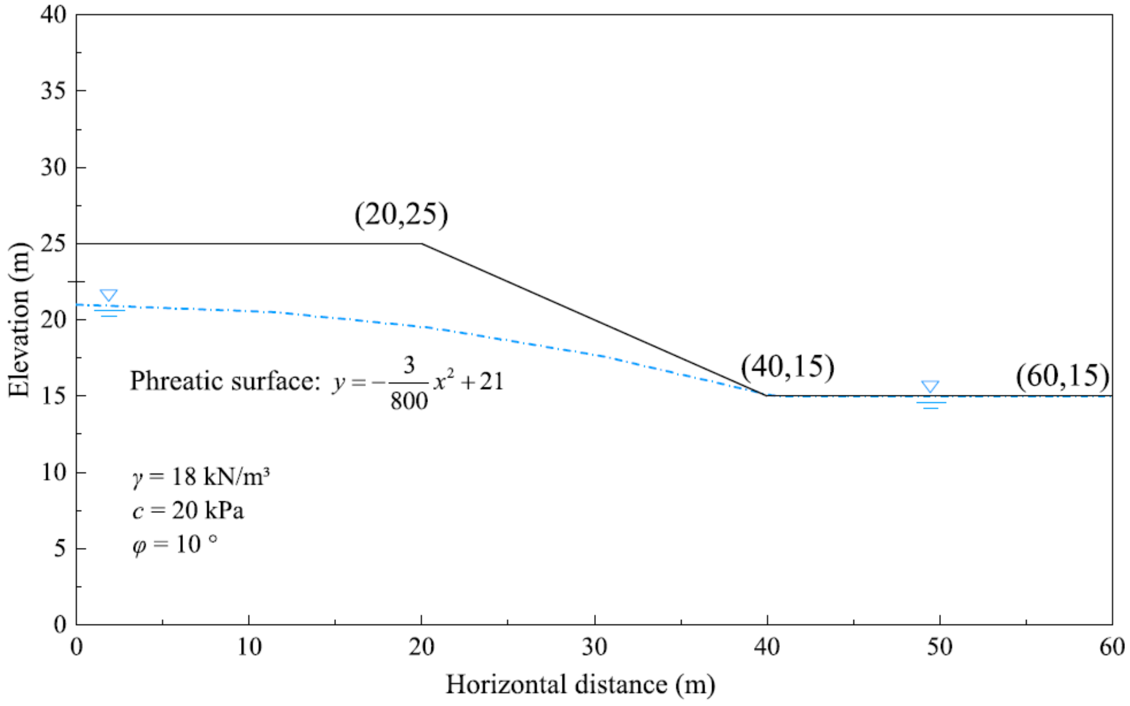

The homogeneous slope model for case study 1.

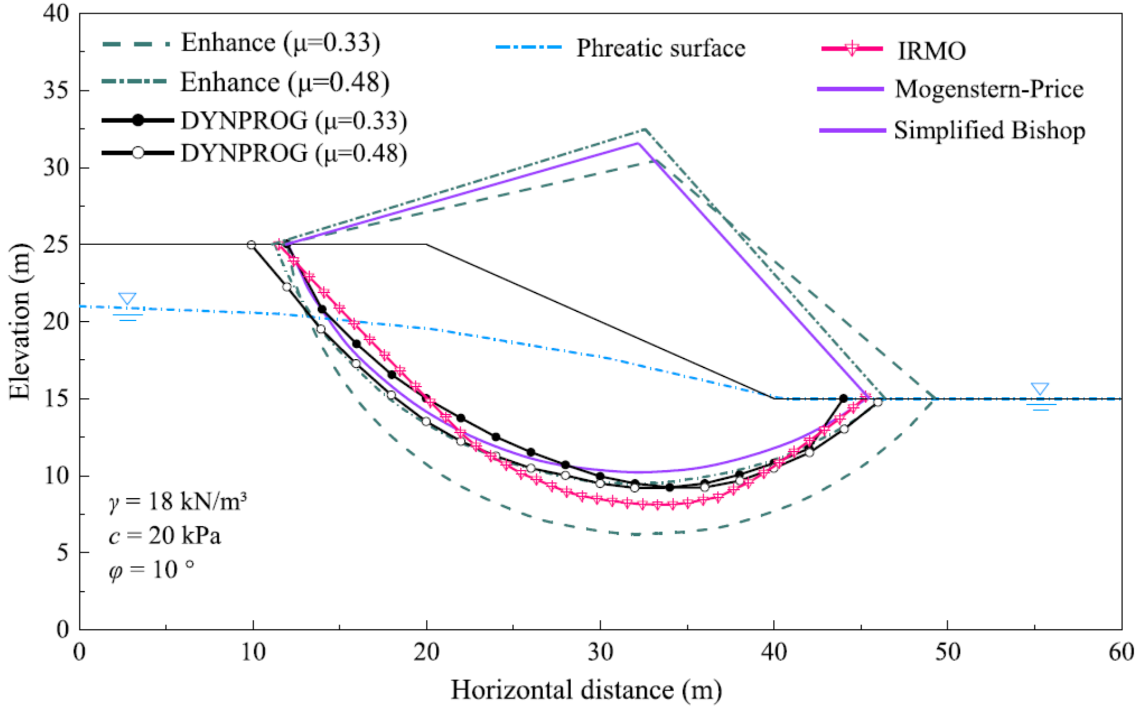

Locations of critical failure surface obtained by various methods for case study 1.

Fs = Factor of safety

The minimum Fs calculated by IRMO is 1.0073, which is much lower (average in -20.6 % lower) than other results.
IRMO has better global searching performance.

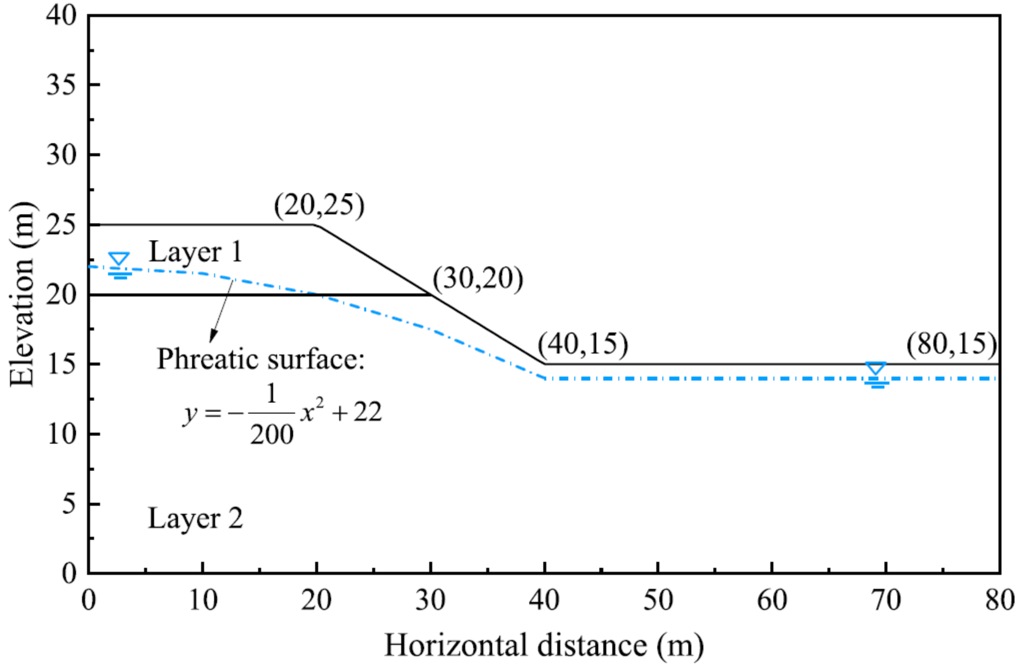

The inhomogeneous slope model for case study 2.

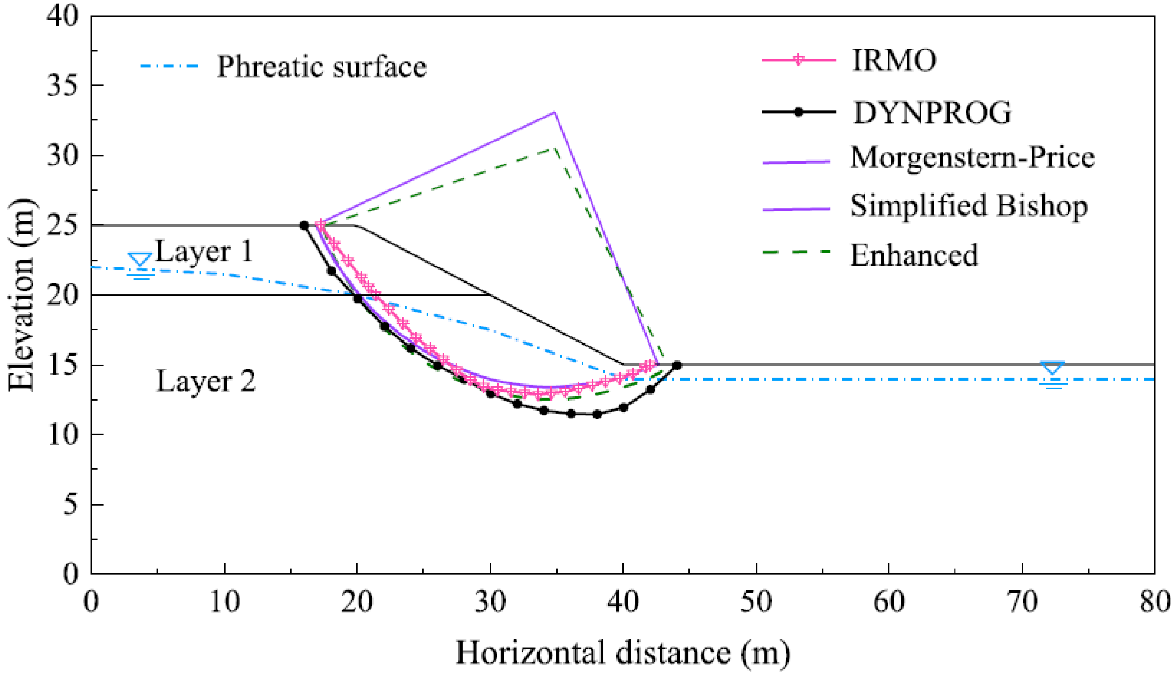

Locations of critical failure surface obtained by various methods for case study 2.

Layer	γ(kN/m^3)	c(kPa)	φ (°)
1	15	5	20
2	18	10	25

The minimum *Fs* calculated by IRMO is 1.353, which is much lower (average in -6.6 % lower) than other results.
IRMO has better global searching performance.

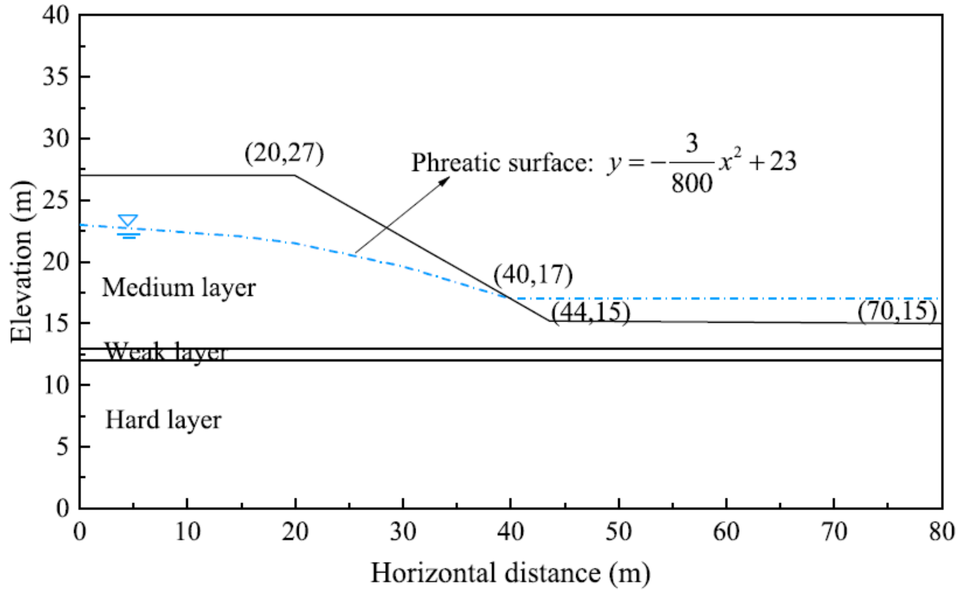

The inhomogeneous slope model for case study 3.

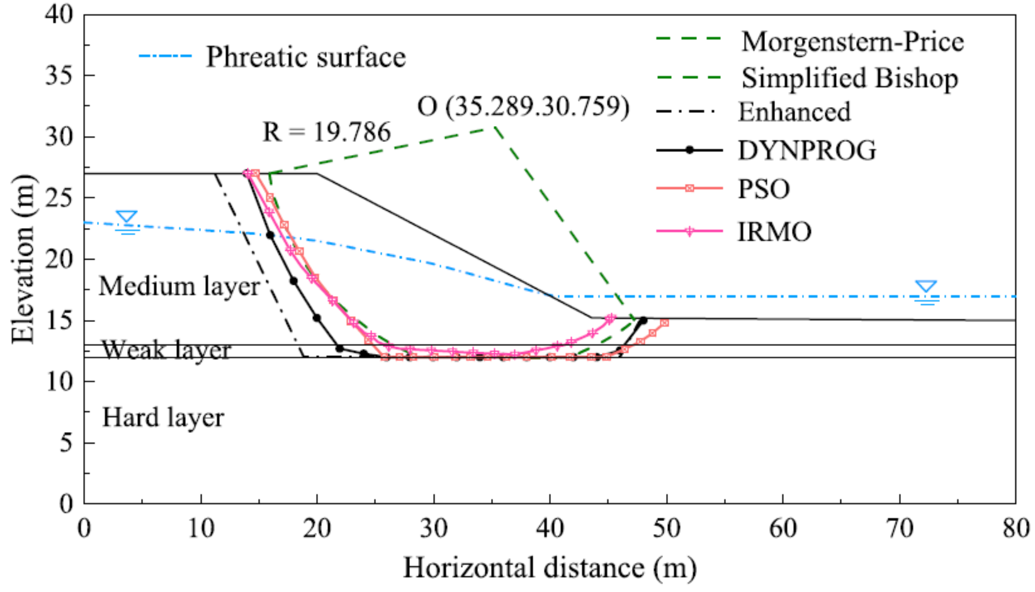

Locations of critical failure surface obtained by various methods for case study 3.

Soil properties of layered slope for case study 3.

Layer	γ(kN/m^3)	c(kPa)	φ (°)
1: Medium layer	15	20	30
2: Weak layer	18	0	10
3: Hard layer	20	100	30

The minimum *Fs* calculated by IRMO is 1.216, which is much lower (average in -9.7 % lower) than other results.
IRMO has better global searching performance.

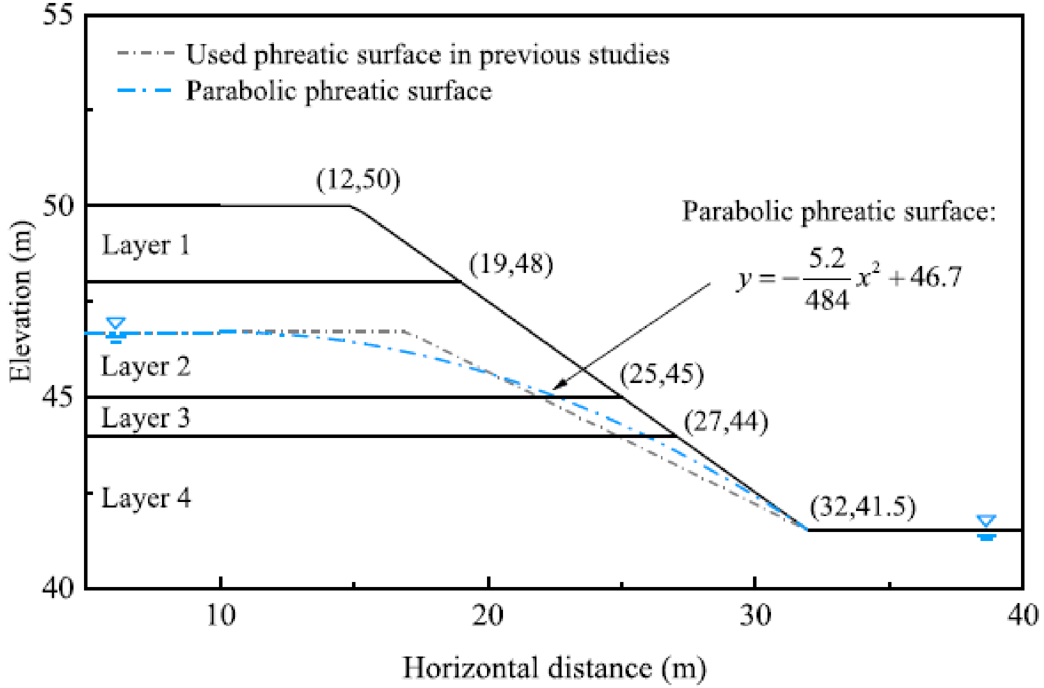

The inhomogeneous slope model for case study 4.

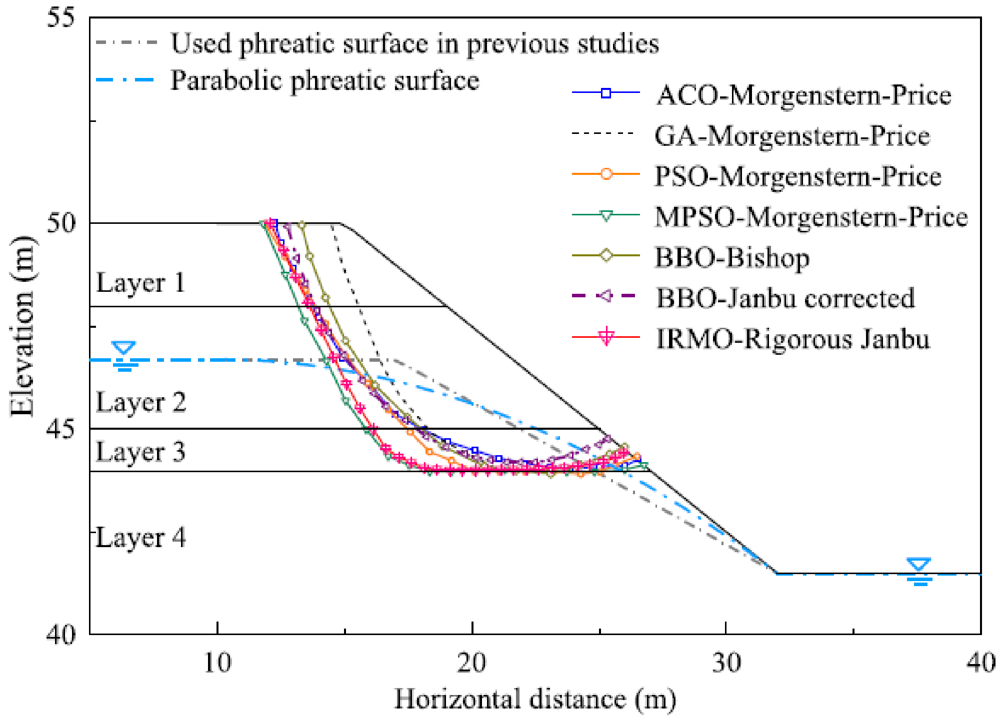

Locations of critical failure surface obtained by various methods for case study 4.

Soil properties of layered slope for case study 4.

Layer	γ (kN/m^3)	c (kPa)	φ (°)
1	19.0	15.0	20.0
2	19.0	17.0	21.0
3	19.0	5.0	10.0
4	19.0	35.0	28.0

The minimum *Fs* calculated by IRMO is 1.052, which is much lower (average in -3.6 % lower) than other results.
IRMO has better global searching performance.

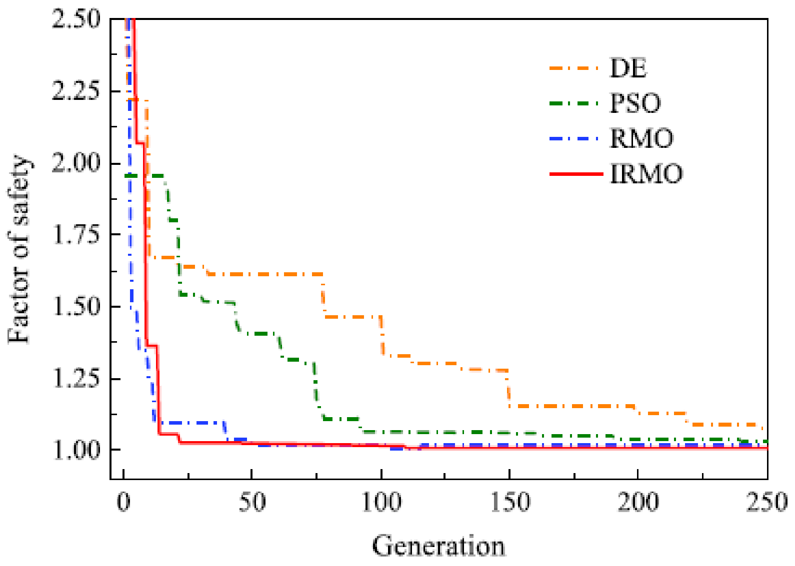

(a) case study 1

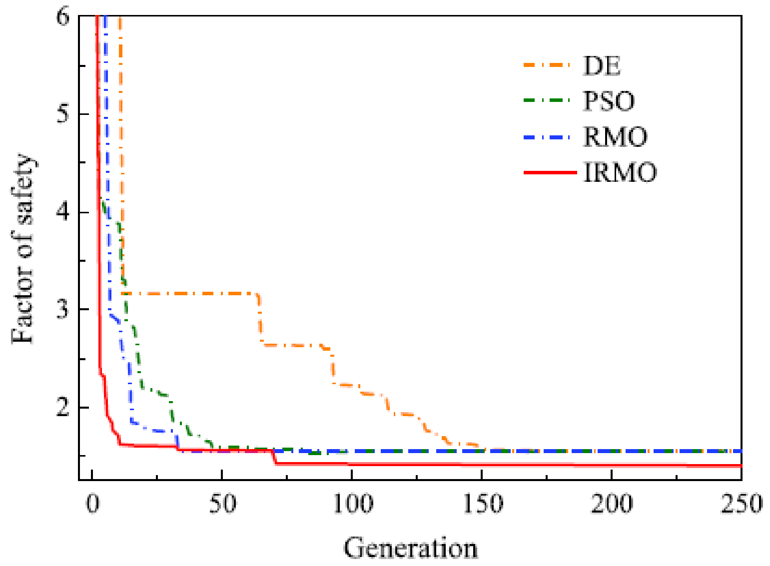

(b) case study 2

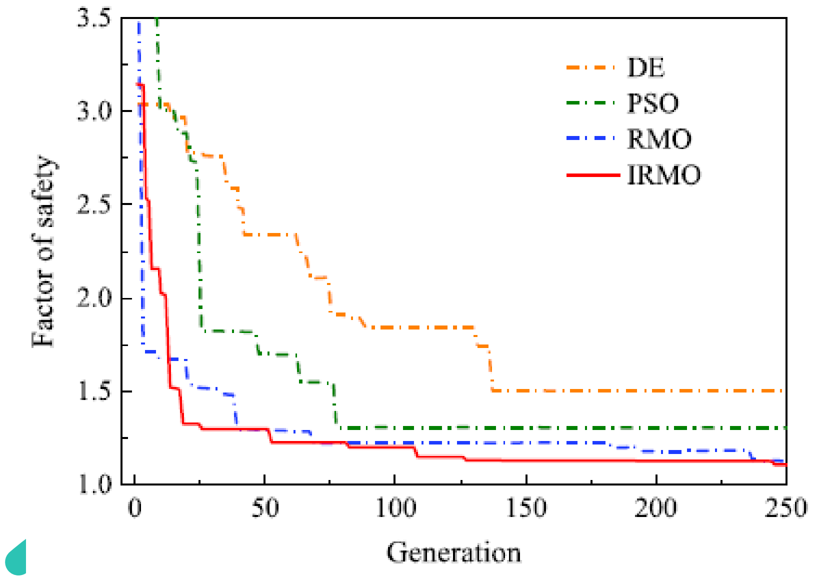

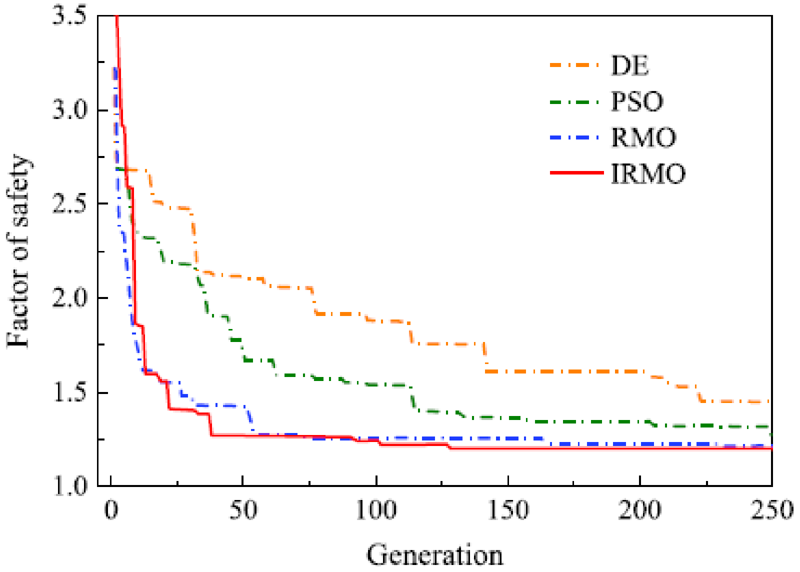

The IRMO algorithm is always the one with the fastest convergence speed and minimum Fs.

Conclusion

- The IRMO shows great applicability and accuracy in implementation for both homogeneous and inhomogeneous slopes by Rigorous Janbu method, which is usually considered difficult to convergence.

- The Rigorous Janbu method of this study could effectively locate the CFS with lower minimum Fs.

- With the advantages of fast convergence, taking up little storage, high stability and simple implementation, the IRMO has appreciable potential to be coupled with FEM methods or embedded in advanced reinforcement learning algorithms for more complex nonlinear stability analysis in the future.

Thanks for listening

Comparison of the minimum *Fs* obtained by different methods for case study 1.

Research	Critical failure surface	Optimization method	Slope stability analysis method	Factor of safety	Error
Pham and Fredlund [63]	Noncircular	FlexPDE	DYNPROG ($\mu = 0.33$)	1.041	−7.4%
	Noncircular	FlexPDE	DYNPROG ($\mu = 0.48$)	1.187	−33.9%
	Circular	SIGMA/W & SEEP/W	Enhanced ($\mu = 0.33$)	1.132	−24.2%
	Circular	SIGMA/W & SEEP/W	Enhanced ($\mu = 0.48$)	1.171	−14.0%
	Circular	SLOPE/W	Morgenstern-Price	1.168	−13.8%
	Circular	SLOPE/W	Simplified Bishop	1.167	−13.7%
Qin [64]	Circular	Fortran	Fellenius	1.070	−12.9%
	Circular	Fortran	Simplified Bishop	1.185	−33.5%
	Circular	Fortran	Rigorous Janbu	1.178	−32.3%
This study	**Noncircular**	**IRMO**	**Rigorous Janbu**	**1.007**	**Average in −20.6%**

Note:*μ is the Poisson's ratio.*

Comparison of the minimum *Fs* for case study 2.

Research	Critical failure surface	Optimization method	Slope stability analysis method	Factor of safety	Error
Pham and Fredlund [63]	Noncircular	FlexPDS	DYNPROG	1.413	−4.2%
	Circular	SIGMA/W & SEEP/W	Enhanced	1.454	−6.9%
	Circular	SLOPE/W	Morgenstern-Price	1.485	−8.9%
	Circular	SLOPE/W	Simplified Bishop	1.483	−8.8%
Qin [64]	Circular	Fortran	Fellenius	1.376	−1.7%
	Circular	Fortran	Bishop	1.489	−9.1%
This study	**Noncircular**	**IRMO**	**Rigorous Janbu**	**1.353**	**Average in −6.6%**

Comparison of the minimum *Fs* for case study 3.

Research	Critical failure surface	Optimization method	Slope stability method	Factor of safety	Error
Pham and Fredlund [63]	Circular	SLOPE/W	Morgenstern-Price	1.140	−7.7%
	Circular	SLOPE/W	Simplified Bishop	1.125	−10.9%
	Circular	SIGMA/W & SEEP/W	Enhanced	1.102	−4.5%
	Noncircular	FlexPDS	DYNPROG	1.000	+5.2%
Chen et al. [62]	Noncircular	PSO & FEM	FEM	1.053	−0.1%
This Study	**Noncircular**	**IRMO**	**Rigorous Janbu**	**1.052**	**Average in −3.6%**

Comparison of the minimum *Fs* using optimization algorithms for case study 4.

Research	Critical failure surface	Optimization method	Slope stability analysis method	Minimum *Fs*	Error
Zolfaghari, et al [23]	Noncircular	GA	Morgenstern-Price	1.360	−10.6%
Cheng, et al [10]	Noncircular	SA	Spencer	1.284	−5.3%
	Noncircular	GA	Spencer	1.232	−1.3%
	Noncircular	PSO	Spencer	1.210	+0.5%
	Noncircular	SHM	Spencer	1.233	−1.4%
	Noncircular	MHM	Spencer	1.225	+0.7%
	Noncircular	Tabu search	Spencer	1.343	−10.44%
	Noncircular	ACO	Spencer	1.449	−16.1%
Kahatadeniya, et al[65]	Noncircular	ACO	Morgenstern-Price	1.377	−11.7%
Khajehzadeh, et al[32]	Noncircular	PSO	Morgenstern-Price	1.203	+1.1%
	Noncircular	MPSO	Morgenstern-Price	1.171	+3.8%
Singh, et al [41]	Circular	BBO	Bishop	1.348	−9.8%
	Circular	BBO	Fellenius	1.226	−0.8%
	Circular	BBO	Janbu	2.103	−42.2%
	Circular	BBO	Janbu corrected	2.104	−42.2%
This Study	**Noncircular**	**IRMO**	**Rigorous Janbu**	**1.216**	**Average in −9.7%**

Comparison of the minimum *Fs* determined by IRMO, RMO, DE and PSO.

	Optimization method	Minimum *Fs*			Standard deviation	Average CPU time (ms)
		Maximum	Minimum	Average		
Case study 1	**IRMO (this study)**	**1.0092**	**1.0042**	**1.0066**	**0.0013**	**755.85**
	RMO	1.0302	1.0116	1.0173	0.0048	713.90
	DE	1.0715	1.0342	1.0571	0.0092	431.30
	PSO	1.0890	1.0293	1.0594	0.0196	2104.05
Case study 3	**IRMO (this study)**	**1.0775**	**1.0412**	**1.0638**	**0.0093**	**665.5**
	RMO	1.1497	1.0341	1.0932	0.0249	643.2
	DE	1.1965	1.1048	1.1395	0.0216	395.9
	PSO	1.2978	1.1138	1.1962	0.0505	2087.6